A GREY-BOX SYSTEM IDENTIFICATION PROCEDURE FOR SCALE MODEL HELICOPTERS BASED ON FREQUENCY-DOMAIN ESTIMATION METHODS

Wei Yuan* , Jay Katupitiya*
***School of Mechanical and Manufacturing Engineering, The University of New South Wales, Sydney**
w.yuan@unsw.edu.au; J.Katupitiya@unsw.edu.au

Keywords: *frequency-domain system identification, scale model helicopters, initial constraints*

Abstract

This paper describes a frequency-domain grey-box system identification procedure for scale model helicopters. It presents a unique way to obtain the initial constraints of the unknown parameters and with this additional information, the identification becomes more efficient. There is no need anymore to start the estimation from blind initial guess or get good starting values through tedious experiments. A well-known 6-DoF LTI MIMO state-space model suitable for hover and near hover condition is used in this paper. In order to identify all the unknown parameters, the model is partitioned into several subsystems in a systematic way. The performance of the proposed procedure is tested in simulations using corrupted flight data by comparing the identified parameters, the eigenvalues and the predicted outputs to their " true" values, respectively.

1 Introduction

Helicopters have significantly complex flight dynamics. They are naturally unstable, nonlinear, highly coupled and multiple-input multiple-output (MIMO) systems. However, the most meaningful non-aggressive applications, such as surveillance and target tracking, are carried out in hover and/or low-speed flight where helicopters can be considered as a LTI MIMO system. This paper presents a systematic system identification procedure to get a sufficiently accurate LTI MIMO dynamic model of the helicopters which is a key step to develop a high-performance unmanned helicopter for hover and/or low-speed flight.

Among various modelling methods, the grey-box system identification has become a popular way to obtain accurate and practical LTI MIMO parametric helicopter models for flight control design. The idea can be generally summarized as a parametric estimation problem, the aim of which is to find values of unknown model parameters λ in a mathematically derived helicopter model, using flight data. The helicopter model is formulated as a MIMO state space model which approximates the nonlinear helicopter dynamics at the chosen operating point. The unknown parameters λ in the model are iteratively determined by minimizing a cost function $J(\lambda)$.

This idea has already been implemented in some commercial software to assist system/parameter identification, e.g. the prediction error method (PEM) in MATLAB System Identification Toolbox [1] and the software package CIFER (Comprehensive Identification from Frequency Responses) [2]. Both of PEM and CIFER start minimizing the cost function $J(\lambda)$ from a set of initial values λ_0 of the model parameters in either time or frequency domain. In order to get an accurate estimation, the values of λ_0 are required to be not too far from the real values of the model parameters P [1], [2]. But Mettler [3, 4, 5], Cai [6] and Peng [7] did not present in detail how they obtained the initial values to start the parameter estimation. Lorenz [8] and Shim [9] used initial guesses to start the identification in their papers. However, the estimation can easily converge to a local minimum of the cost function $J(\lambda)$ or even diverge [9]. One popular and reliable way to obtain good initial values is based on the first-principle modeling [2, 10, 11]. But numerous experiments and measurements are needed to get these values and it is too cumbersome and time consuming.

In order to get good initial values or reliable distribution intervals of the dominant parameters, a practical and efficient way to find these initial constraints was presented in our previous work [12]. A comparison of the estimation convergence with and without the initial constraints was also presented there. With the help of these initial constraints, the partitioned time-domain system identification that we proposed [12] started without effort and identified the linear helicopter hover model successfully.

Since frequency domain analysis has several advantages [13] over that in time domain, including physical insight of the system dynamics within the interested frequency ranges, better robustness against data biases and noises, and fewer number of data points needed for parameter estimation, it is well worth transforming our time-domain method [12] to frequency domain in order to have a better performance, which is to be presented in this paper.

The paper is organized as follows. Section 2 presents the details of the system identification. Section 2.2 presents the linearized helicopter model in hover and near hover flight mode. Section 2.3 gives a brief view of frequency domain estimation algorithms. Section 2.4 contains the systematic identification procedure together with the analysis of the initial constraints, whereas section 3 gives the estimation results and time domain validation. Finally, some conclusions are drawn in section 4.

2 Identification Process

2.1 Flight Data

The essential element of the system identification of a helicopter is collecting flight data during specially piloted open-loop experiments which are aimed to excite the dynamics of interest. The frequency sweeps technique [13] is applied to collect data in our simulations.

As the estimation is to be done in frequency domain, the collected flight data need to be transformed from the time domain to frequency domain first using the Fast Fourier Transformation (FFT).

2.2 Model Structure

As mentioned above, helicopters are naturally nonlinear, unstable and highly coupled, but the hover dynamics can be linearized as a LTI MIMO state space model at the trimmed point. The widely published LTI MIMO state space model structure proposed in [3] is used as the model structure to capture the majority of the system dynamics from the flight data:

$$\dot{x} = Ax + Bu \quad \text{and} \tag{1}$$

$$y = Cx, \tag{2}$$

where $x = [u\ v\ p\ q\ \Phi\ \Theta\ a\ b\ w\ r\ r_{fb}]^T$ is the state vector with u, v, w as the longitudinal, lateral and vertical velocities, respectively; p, q, r as the roll, pitch and yaw rates, respectively; a, b as the longitudinal and lateral flapping angles, respectively with Φ and Θ as roll and pitch angles, respectively. The control input, or the stick inputs is $u = [\delta_{lat}\ \delta_{lon}\ \delta_{col}\ \delta_{ped}]^T$ where the elements in the order are: roll rate control, pitch rate control, collective pitch rate control and the yaw rate control. The output vector is, $y = [u\ v\ w\ p\ q\ r\ \Phi\ \Theta]^T$.

The matrices A and B in Eq. (1) are:

$$A = \begin{bmatrix} X_u & 0 & 0 & 0 & 0 & -g & -g & 0 & 0 & 0 & 0 \\ 0 & Y_v & 0 & 0 & g & 0 & 0 & g & 0 & 0 & 0 \\ L_u & L_v & 0 & 0 & 0 & 0 & L_a & L_b & 0 & 0 & 0 \\ M_u & M_v & 0 & 0 & 0 & 0 & M_a & M_b & 0 & 0 & 0 \\ 0 & 0 & 1 & 0 & 0 & 0 & 0 & 0 & 0 & 0 & 0 \\ 0 & 0 & 0 & 1 & 0 & 0 & 0 & 0 & 0 & 0 & 0 \\ 0 & 0 & 0 & -1 & 0 & 0 & \frac{-1}{\tau_a} & A_b & 0 & 0 & 0 \\ 0 & 0 & -1 & 0 & 0 & 0 & B_a & \frac{-1}{\tau_a} & 0 & 0 & 0 \\ 0 & 0 & 0 & 0 & 0 & 0 & Z_a & Z_b & Z_w & Z_r & 0 \\ 0 & 0 & N_p & 0 & 0 & 0 & 0 & 0 & N_w & N_r & N_{rf} \\ 0 & 0 & 0 & 0 & 0 & 0 & 0 & 0 & 0 & K_r & K_{rf} \end{bmatrix} \quad (3)$$

$$B = \begin{bmatrix} 0 & 0 & 0 & 0 \\ 0 & 0 & 0 & 0 \\ 0 & 0 & 0 & 0 \\ 0 & 0 & 0 & 0 \\ 0 & 0 & 0 & 0 \\ 0 & 0 & 0 & 0 \\ A_{lat} & A_{lon} & 0 & 0 \\ B_{lat} & B_{lon} & 0 & 0 \\ 0 & 0 & Z_{col} & 0 \\ 0 & 0 & N_{col} & N_{ped} \\ 0 & 0 & 0 & 0 \end{bmatrix}. \quad (4)$$

2.3 Estimation Algorithms

With the fixed model structure (Eq. (1) and (2)), the unknown parameters in the matrices A and B are to be estimated by minimizing the cost function $J(\lambda)$ by tuning the model parameter λ:

$$J(\lambda) = N \sum_{k=0}^{N-1} \tilde{\nu}^{\dagger}(k,\lambda)\hat{S}_{\nu\nu}^{-1}(k,\lambda)\tilde{\nu}(k,\lambda), \quad (5)$$

where N is the total number of data points, $\tilde{\nu}(k,\lambda)$ are the residuals between the real and predicted values in frequency domain, $\tilde{\nu}^{\dagger}(k,\lambda)$ is the complex conjugate transpose of $\tilde{\nu}(k,\lambda)$, $\hat{S}_{\nu\nu}(k,\lambda)$ is the power spectral densities of $\tilde{\nu}$

$$\hat{S}_{\nu\nu}(k,\lambda) = \sum_{k=0}^{N-1} \tilde{\nu}(k,\lambda)\tilde{\nu}^{\dagger}(k,\lambda) \quad (6)$$

In some rows in the state-space model (Eq. (1)) which has a generalized form

$$z = \sum_{j=1}^{n} \bar{\lambda}_j^a x_j + \sum_{j=1}^{n} \bar{\lambda}_j^b u_j, \quad (7)$$

the related states x_j, in addition to the inputs u_j, are all measured. The term on the left side z is either measured or can be found from numerical differentiation. In this case, the residuals $\tilde{\nu}(k,\lambda)$ in Eq. (5) are equal to the equation error

$$\tilde{\nu}(k,\lambda) = z - \sum_{j=1}^{n} \lambda_j^a x_j - \sum_{j=1}^{n} \lambda_j^b u_j \quad (8)$$

where $k = 0, 1, ..., N-1$.
So the frequency-domain equation error method (FEEM) here is essentially a least-squares estimation, which doesn't require any starting value [14] but can be only applied to one row at a time, where the states x, the inputs u and the term z on both sides of the equations are known.

But not all of the states and their derivatives in a state space model are usually known. In this case, only the data from the output equation (Eq. (2)) and input data are available. The estimation problem is to minimize the error between the measured and predicted outputs with the same input data. The residuals $\tilde{\nu}(k,\lambda)$ in Eq. (5) are then equal to the output error between model output $y(k)$ and measured output $z(k)$ in frequency domain

$$\tilde{\nu}(k,\lambda) = z(k) - y(k) \quad (9)$$

where $k = 0, 1, ..., N-1$.
This frequency-domain output error method (FOEM) is one of the most used maximum likelihood parameter estimation methods for LTI MIMO aircraft dynamic systems [2, 4, 13].

The toolbox, SIDPAC (System Identification Programs for Aircraft) [13] is used here to perform the frequency domain estimation methods. More details about the FEEM and FOEM can be found there.

2.4 Partitioned System identification Procedure

There are more than 30 unknown parameters in Eq. (1) to be identified. It is impractical to estimate all the parameters in one go. So the partitioned system identification procedure proposed in our previous work [12] is adopted here with minimal modification and our attention will be paid to those key parameters that are dominant in the dynamics of each subsystem.

The partitioned systems include lateral translational dynamics, roll dynamics, longitudinal translational dynamics, pitch dynamics, heave dynamics and yaw dynamics. In each subsystem, the initial constraints are to be discussed based on the physical insight of the helicopter system and flight data. They prevent the estimators from calculating the cost functions in some parameter ranges where no reasonable physical meanings exists. Besides, the FEEM is used in some equations to obtain some suitable initial values from measured and input data. Given all the *a priori* information from above, the FOEM can start reliable parameter estimations. Note that the initial constraints of all the cross coupling parameters are not discussed in detail but simply set to 0. So the estimated cross coupling parameters may be not around their "true" values. However, they are not the dominant parameters that capture the main dynamics of each subsystem.

The positive directions of the helicopter coordinate and controller inputs are shown in Fig. 1. They are of importance to understand the correct motions from recorded flight data.

2.4.1 Lateral translational dynamics

$$\dot{v} = Y_v v + g\Phi + gb \tag{10}$$

Y_v is the speed force damping derivative in Y-direction and physically should be a negative value, $(Y_v < 0)$ and g is equal to the acceleration of gravity. When exciting the helicopter with low frequency lateral input, the flapping dynamics can be ignored, i.e., the term gb in (10) can be ignored. So the only unknown parameter here is Y_v. Since v and Φ are the collected flight data and

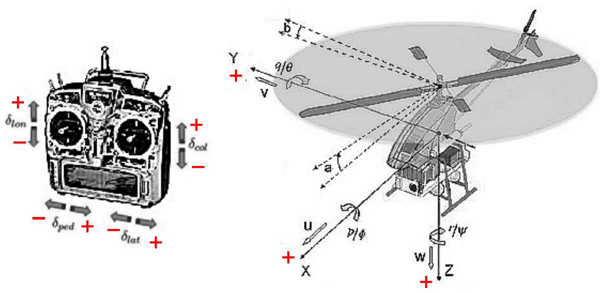

Fig. 1 Definition of coordinate and controller inputs (modified from [15])

.

$\dot{v}$ can be derived from the data set v, the FEEM can be used to estimate the parameter Y_v which is to be taken as its starting value in the next iteration.

2.4.2 Roll dynamics

$$\begin{bmatrix} \dot{v} \\ \dot{p} \\ \dot{\Phi} \\ \dot{b} \end{bmatrix} = \begin{bmatrix} Y_v & 0 & g & g \\ L_v & 0 & 0 & L_b \\ 0 & 1 & 0 & 0 \\ 0 & -1 & 0 & \frac{1}{\tau_a} \end{bmatrix} \begin{bmatrix} v \\ p \\ \Phi \\ b \end{bmatrix} + \begin{bmatrix} 0 \\ 0 \\ 0 \\ B_{lat} \end{bmatrix} \delta_{lat} \tag{11}$$

In Eq.11, L_v describes how the helicopter's roll dynamics response to an increase in v. As a wind gust from left side causes a positive rolling motion, L_v has a positive sign, $(L_v > 0)$. B_{lat} is the gain from the lateral input to the roll dynamics with a positive sign, $(B_{lat} > 0)$. τ_a is the time constant that is due to the stabilizer bar. Shim shows in [9] that the time constant τ_a expressed in seconds can be roughly calculated with $\tau_a = \frac{5}{\Omega_R/60}$, where Ω_R is the main rotor speed expressed in rpm. For the helicopter model used in this paper, τ_{a0} = 0.3333. This value will be used as the starting value to estimate τ_a. As the main rotor typically has a very fast dynamic response, its time constant should also be within the range $(0 < \tau_a < 1)$.

L_b represents the roll rotor spring coefficient and its square root $\sqrt{L_b}$ is close to the rolling mode frequency of the vehicle [3], which also relates to the frequency where the frequency response of $\frac{p}{\delta_{lat}}$ reaches its peak. Since the data p and δ_{lat} are known, it's easy to get the plot of the frequency response of $\frac{p}{\delta_{lat}}$ (Fig. 2) [14]. So a certain range for L_b can be given as $(120 < L_b < 180)$.

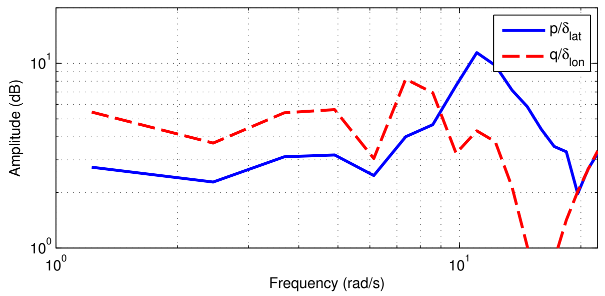

Fig. 2 Frequency response of $\frac{p}{\delta_{lat}}$ and $\frac{q}{\delta_{lon}}$

The output data p and v and the input signal δ_{lat} are put into the FOEM to estimate the unknown parameters L_v, L_b, τ_a and B_{lat} with their constraints and also refine Y_v.

2.4.3 Longitudinal translational dynamics

$$\dot{u} = X_u u - g\Theta - ga \tag{12}$$

X_u is the speed force damping derivative in x-direction $(X_u < 0)$. Similar to (10), it is the only one to be estimated using the FEEM.

2.4.4 Pitch dynamics

$$\begin{bmatrix} \dot{u} \\ \dot{q} \\ \dot{\Theta} \\ \dot{a} \end{bmatrix} = \begin{bmatrix} X_u & 0 & -g & -g \\ M_u & 0 & 0 & M_a \\ 0 & 1 & 0 & 0 \\ 0 & -1 & 0 & \frac{-1}{\tau_a} \end{bmatrix} \begin{bmatrix} u \\ q \\ \Theta \\ a \end{bmatrix} + \begin{bmatrix} 0 \\ 0 \\ 0 \\ A_{lon} \end{bmatrix} \delta_{lon} \tag{13}$$

Similar to L_b in Eq.11, above M_a is the pitch rotor spring coefficient and its square root $\sqrt{M_a}$ is close to the pitching mode frequency of the vehicle. From the frequency response of $\frac{q}{\delta_{lon}}$ (Fig.2), the range for M_a is $(50 < M_a < 90)$.

M_u describes how the helicopter's pitch dynamics responses to an increase in u. If the helicopter experiences a wind gust from back, it has a negative pitching motion and therefore $M_u < 0$. A_{lon} is the gain from the longitudinal input to the pitch dynamics $(A_{lon} < 0)$.

Similar to the estimation of roll dynamics, the output data q and u and the input signal δ_{lon} are used to estimate the unknown parameters M_u, M_a and A_{lon} with their constraints and refine X_u and τ_a which should not change too much from their starting values.

2.4.5 Coupled longitudinal and lateral dynamics

The two subsystems (11) and (13) are combined to form the coupled longitudinal-lateral model which is the same as the first 8 rows of Eq. (1).

The parameters identified in the previous steps are to be refined here, after adding the cross-coupling parameters L_a, M_b, A_b, B_a, L_u, M_v, A_{lat} and B_{lon} to the model. The initial values of these cross-coupling parameters are all set to 0. The FOEM uses a set of flight data that is excited by two inputs δ_{lat} and δ_{lon} simultaneously to do the estimation.

2.4.6 Heave dynamics

$$\dot{w} = Z_a a + Z_b b + Z_w w + Z_r r + Z_{col}\delta_{col} \tag{14}$$

Z_a and Z_b describe the cross coupling effects from flapping dynamics to heave channel and Z_r is the effect from yaw rate changes. They are excluded from the above equation in order to get the dominant heave model $\dot{w} = Z_w w + Z_{col}\delta_{col}$. The parameters Z_w and Z_{col} can be obtained via the FEEM. Z_w represents the heave damping $(Z_w < 0)$. Z_{col} is the gain from the collective input to the heave dynamics $(Z_{col} < 0)$.

2.4.7 Yaw dynamics

$$\begin{bmatrix} \dot{r} \\ \dot{r}_{fb} \end{bmatrix} = \begin{bmatrix} N_r & N_{rf} \\ K_r & K_{rf} \end{bmatrix} \begin{bmatrix} r \\ r_{fb} \end{bmatrix} + \begin{bmatrix} N_{ped} \\ 0 \end{bmatrix} \delta_{ped} \tag{15}$$

A feedback yaw rate gyro is installed on the helicopter and the yaw rate feedback r_{fb} provides negative yaw rate compensation to enhance the yaw stability. K_r is the yaw rate feedback gain without the minus sign $(K_r > 0)$.

N_r represents the yaw damping coefficient $(N_r < 0)$. N_{ped} is the gain from the yaw rate control input to the yaw dynamics $(N_{ped} > 0)$. Additionally, there are still two extra constraints $N_{rf} = -N_{ped}$ and $K_{rf} = 2N_r$ suggested in [3, 4].

Taking all the constraints just mentioned above, the FOEM is to estimate the unknown parameters N_r, N_{ped}, K_r, N_{rf} and K_{rf} by using the measured yaw rate r and the yaw rate control signal δ_{ped}.

2.4.8 Coupled heave-yaw dynamics

The two subsystems (14) and (15) are combined to form the coupled heave-yaw model which is the same as the last 3 rows of Eq. (1).

The parameters estimated in the last two steps are to be refined here, while two heave-to-yaw coupling parameters (N_w and N_{col}) and one yaw-to-heave coupling parameter (Z_r) are to be estimated. The initial values of the coupling parameters are set to 0. A set of data with two inputs δ_{col} and δ_{ped} is put into FOEM.

2.4.9 Complete dynamic model

The coupled longitudinal-lateral model and the coupled heave-yaw model are combined as the complete model structure (1) with two further cross-coupling parameters Z_b and N_p. The parameter Z_a is fixed to 0, because its original value in the "true" plant was set to 0.

All the input data (δ_{lat}, δ_{lon}, δ_{col}, δ_{ped}) and output data (u, v, w, p, q, r Φ, Θ) are put into the FOEM to run the final estimation where the initial values of Z_b and N_p are set to 0.

The final step of the entire estimation procedure is to refine all the parameters determined with a new set of flight data. The changes of the estimated values should be small, especially the on-axis parameters.

3 Results in Simulations

The Yamaha R-50 model in [9] is used as the "true" platform in simulations to perform hover flight with a quasi-constant rotor speed of 900 RPM. Although the model simplifies the real life situation, it describes the hover dynamics, which is dominant in low frequency, well. The model shares the same system equation as Eq. (1). But the output data are substantially corrupted with certain Gaussian white noises and constant biases which are very common in the real life situation:

$$\dot{x} = Ax + Bu \quad \text{and} \qquad (16)$$
$$y = Cx + Nw + Gd, \qquad (17)$$

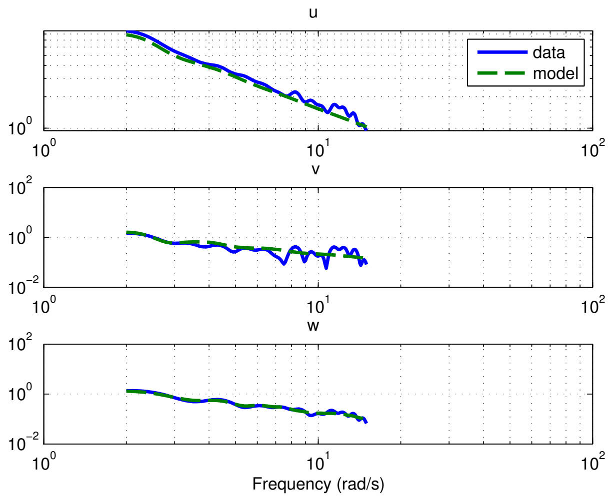

Fig. 3 Identification results for u, v and w.

where w are the measurement noises and d the measurement biases. The matrices N and G are diagonal matrices with weights along the diagonal that can be adjusted to add noise and bias.

The parameter values of the "true" platform are listed in column “real ” value in Table 1. The acceleration due to gravity g is a known parameter and is set at 32.2 ft/s^2. Note that Shim [9] used imperial units in his original work, but he didn’t clearly indicate the unit of each parameter listed in the column. In order to avoid incorrect converting, we keep the original units in this example.

3.1 Frequency Response

Fig.3 to 5 show the frequency-domain identification results from the partitioned system identification procedure. Note that the outputs of the "true" system have been corrupted by noises of high-frequency and constant biases. But they can be easily eliminated from the data in frequency domain by selecting a suitable frequency range that only includes the relevant information in the data. Fig.3 to 5 indicate that the model outputs fit to the "true" data in the frequency range where the hover dynamics is dominant.

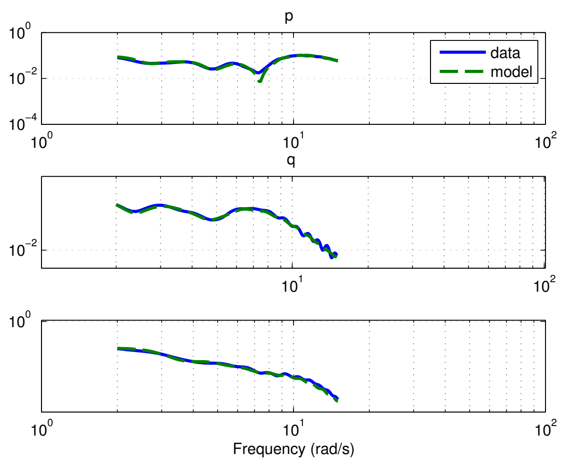

Fig. 4 Identification results for p, q and r.

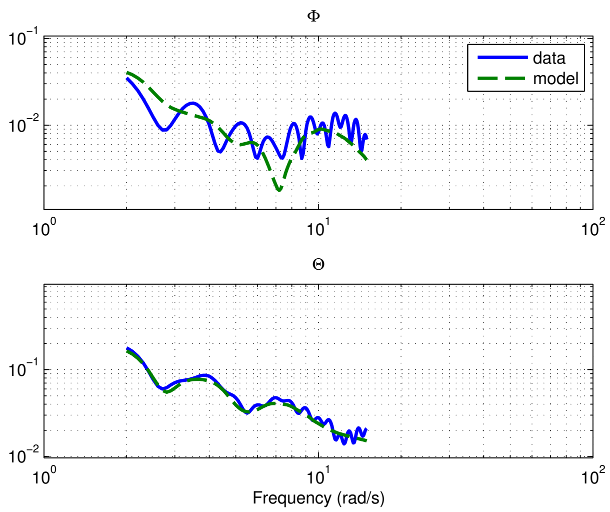

Fig. 5 Identification results for Φ and Θ.

3.2 Parameter Estimation

The mean values of the identified parameters are listed in Table.1. Although it is popular to use Cramer Rao Bound(CR%) and Insensitivity (I%) [2, 4] or standard error [16, 17] to indicate the estimation accuracy, they don't indicate the difference between the estimates and the true values. As the values of the "true" parameters are known in this example, it is more reasonable to compare the identified values to the real model parameters. The estimation of the key parameters mentioned in last section has achieved a high accuracy level, while the estimation of the cross-coupling parameters is slightly worse as expected but still good.

(a) A-Matrix

	"real"	est
X_u	-0.13	-0.12
Y_v	-0.42	-0.39
L_u	-0.18	-0.15
L_v	0.09	0.07
L_a	36.71	47.43
L_b	161.11	160.25
M_u	-0.08	-0.06
M_v	-0.05	-0.06
M_a	63.58	63.30
M_b	-19.49	-18.58
τ_a	0.29	0.28
A_b	0.83	0.81
B_a	0.36	0.31
Z_b	9.64	7.78
Z_w	-0.76	-0.76
Z_r	8.42	8.33
N_p	-1.33	-0.92
N_w	0.06	0.06
N_r	-5.51	-5.51
N_{rf}	-44.87	-43.65
K_r	1.80	1.81
K_{rf}	-11.02	-11.02

(b) B-Matrix

	"real"	est
A_{lat}	-0.84	-0.85
A_{lon}	-2.82	-2.83
B_{lat}	2.41	2.45
B_{lon}	-0.35	-0.25
Z_{col}	-70.50	-71.20
N_{col}	23.63	24.12
N_{ped}	44.87	43.65

Table 1 Parameter Identification

3.3 Eigenvalues

As the eigenvalues represent the dynamic modes and the essential characteristics of a system, a comparison of the eigenvalues of the original model and the identified one would be a more intuitive way to assess the accuracy of the estimation. Fig.6 shows that the eigenvalues of the identified model are all close to the original ones, which means the model is able to describe the characteristics of the system. In other words, the model is able to predict the system's responses, which is shown in the next subsection.

3.4 Model Validation

To validate the prediction performance of the identified model, the model is excited with the control input data from another set of flight data which is not used in the identification part above. The predicted helicopter responses are compared with the "real" outputs in time domain. The com-

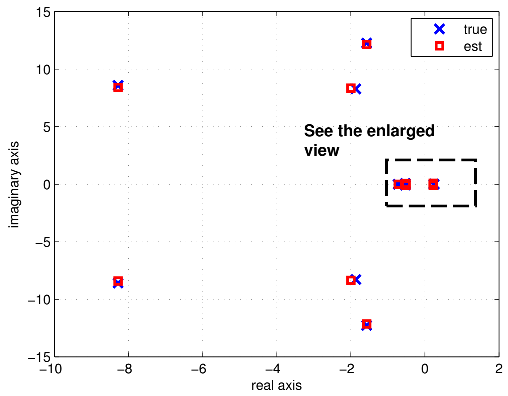

Fig. 6 Eigenvalues.

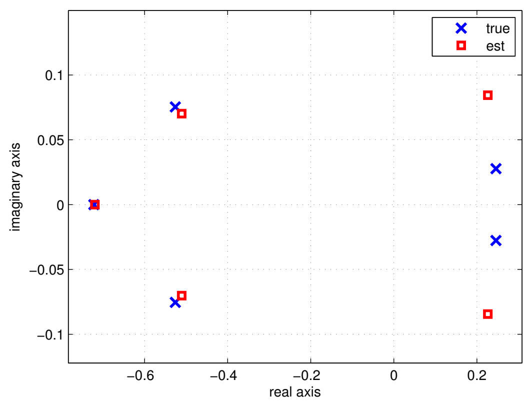

Fig. 7 Enlarged View of selected zone in Fig. 6.

parison is shown in Fig. 8 - 10. For the comparison purpose, the "real" flight data here are the clear data without noises and biases. It shows an excellent agreement with the original system for all channels for about 8 seconds. The differences between the "real" and predicted values in some channels, u, v, q, Φ and Θ, increase in the last c.a. 2 seconds. The reason is that the platform shows the unstable status around that time. According to the eigenvalues of the system 7, the helicopter has a pair of unstable eigenvalues. But the unstable eigenvalues of the identified model are a little away from the "true" values. It causes the differences of the outputs there. However, the agreement is still satisfactory.

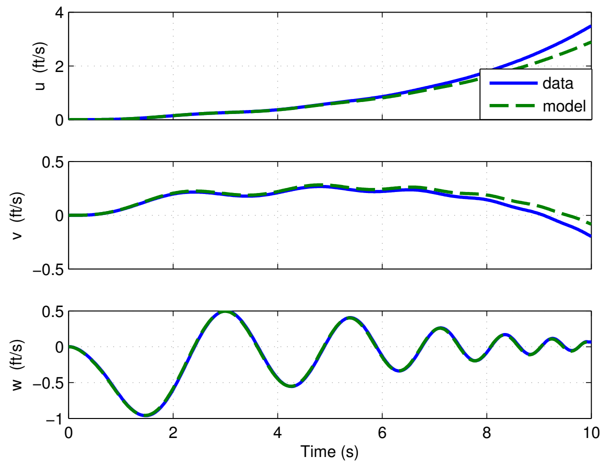

Fig. 8 Validation by translational velocity prediction.

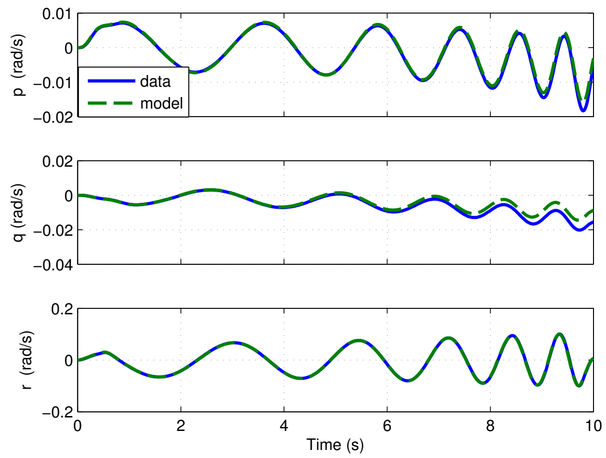

Fig. 9 Validation by rotational rate prediction.

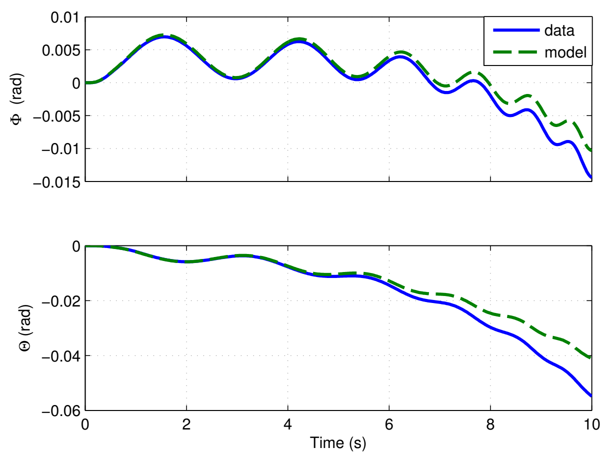

Fig. 10 Validation by roll and pitch prediction.

4 Conclusions

A frequency domain grey-box system identification procedure suitable for scale-model helicopters operating in hover and near hover condition has been described. In order to make the system identification more efficient, a set of initial constraints has been found and added to the partitioned system identification procedure based on the FEEM and FOEM. The approach does not need cumbersome first principle modeling to obtain suitable initial values or blind guesses to start estimations. In the simulation case, the proposed procedure has successfully identified the hover model with high accuracy from flight data which were corrupted with noises and biases. In the future work, the proposed system identification will be further tested and validated using real flight data.

References

[1] L. Ljung, *System Identification Toolbox User's Guide*. The Math Works, Inc, 2003.

[2] M. B. Tischler and R. K. Remple, *Aircraft and Rotorcraft System Identification: Engineering Methods with Flight Test Examples*. American Institute of Aeronautics and Astronautics, 2006.

[3] B. Mettler, M. B. Tischler, and T. Kanade, "System identification of small-size unmanned helicopter dynamics," in *American Helicopter Society 55th Forum, Montreal, Quebec, Canada*, 1999.

[4] B. Mettler, *Identification Modeling and Characteristics of Miniature Rotorcraft*. Kluwer Academic Publishers, 2003.

[5] B. Mettler, M. B. Tischler, and T. Kanade, "System identification modeling of a small-scale unmanned rotorcraft for flight control design," *Journal of the American Helicopter Society*, vol. 47, pp. 50 –63, 2002.

[6] G. Cai, B. M. Chen, K. Peng, M. Dong, and T. H. Lee, "Modeling and control system design for a uav helicopter," in *Proc. 14th Mediterranean Conf. Control and Automation MED '06*, 2006, pp. 1–6.

[7] K. Peng, G. Cai, B. M. Chen, M. Dong, K. Y. Lum, and T. H. Lee, "Design and implementation of an autonomous flight control law for a uav helicopter," *Automatica*, vol. 45, no. 10, pp. 2333 – 2338, 2009.

[8] S. Lorenz and G. Chowdhary, "Non-linear model identification for a miniature rotorcraft preliminary results," in *61st Annual Forum Proceedings - AHS International*, vol. 2, 2005, pp. 1647–1660.

[9] H. Shim, "Hierarchical flight control system synthesis for rotorcraft-based unmanned aerial vehicles," Ph.D. dissertation, UNIVERSITY OF CALIFORNIA, BERKELEY, 2000.

[10] S. Bhandari, "Flight validated high-order models of uav helicopter dynamics in hover and forward flight using analytical and parameter identification techniques," Ph.D. dissertation, University of Kansas, 2007.

[11] A. Budiyono, K. J. Yoon, and F. D. Daniel, "Integrated identification modeling of rotorcraft-based unmanned aerial vehicle," in *Proc. 17th Mediterranean Conf. Control and Automation MED '09*, 2009, pp. 898–903.

[12] W. Yuan and J. Katupitiya, "A time-domain grey-box system identification procedure for scale-model helicopters," in *Proceedings of the 13th Australian Conference on Robotics and Automation*, Melbourne, Australia, 2011.

[13] V. Klein and E. A. Morelli, *Aircraft System Identification: Theory and Practice*. AIAA, 2006.

[14] L. Ljung, *System identification : theory for the user*, 2nd ed. Upper Saddle River, NJ : Prentice Hall PTR, 1999.

[15] G. Cai, B. M. Chen, X. Dong, and T. H. Lee, "Design and implementation of a robust and nonlinear flight control system for an unmanned helicopter," *Mechatronics*, vol. 21, no. 5, pp. 803 – 820, 2011, special Issue on Development of Autonomous Unmanned Aerial Vehicles.

[16] E. A. Morelli, "System identification programs for aircraft (sidpac)," in *AIAA Atmospheric Flight Mechanics Conference*, 2002.

[17] J. Grauer, J. Conroy, J. H. Jr., J. Humbert, and D. Pines, "System identification of a miniature helicopter," *Journal of Aircraft*, vol. vol.46 no.4, pp. 1260–1269, 2009.

Copyright Statement